



ERK signaling expands mammalian cortical radial glial cells and extends the neurogenic period

Mengge Sun^{a,1} , Yanjing Gao^{a,1}, Zhenmeiyu Li^a, Lin Yang^a, Guoping Liu^a , Zhejun Xu^a , Rongliang Guo^a , Yan You^a, and Zhengang Yang^{a,2}

Edited by Nenad Sestan, Yale University School of Medicine, New Haven, CT; received September 1, 2023; accepted February 12, 2024 by Editorial Board Member Jeremy Nathans

The molecular basis for cortical expansion during evolution remains largely unknown. Here, we report that fibroblast growth factor (FGF)-extracellular signal-regulated kinase (ERK) signaling promotes the self-renewal and expansion of cortical radial glial (RG) cells. Furthermore, FGF-ERK signaling induces *bone morphogenic protein 7* (*Bmp7*) expression in cortical RG cells, which increases the length of the neurogenic period. We demonstrate that ERK signaling and Sonic Hedgehog (SHH) signaling mutually inhibit each other in cortical RG cells. We provide evidence that ERK signaling is elevated in cortical RG cells during development and evolution. We propose that the expansion of the mammalian cortex, notably in human, is driven by the ERK-BMP7-GLI3R signaling pathway in cortical RG cells, which participates in a positive feedback loop through antagonizing SHH signaling. We also propose that the relatively short cortical neurogenic period in mice is partly due to mouse cortical RG cells receiving higher SHH signaling that antagonizes ERK signaling.

cortical evolution | FGF signaling | ERK signaling | BMP7 | SHH

Insights into the evolution of the human cerebral cortex are beginning to come to light (1–7). Early human cortical development is driven by four types of neural stem cells which are the source for cortical glutamatergic pyramidal neurons (PyNs) and glia: ventricular zone (VZ) neuroepithelial cells, VZ full span radial glial (fRG) cells, VZ truncated radial glial (tRG) cells, and outer radial glial (oRG, also known as basal RG) cells which lie in the outer subventricular zone (outer SVZ, OSVZ) (4, 7–15). Human cortical neuroepithelial cells start to convert into fRG cells around gestational week 7 (GW7), and fRG cells give rise to oRG and tRG cells around GW16 (11, 12, 16). We recently provided evidence that oRG cells in the cortical OSVZ are mainly neurogenic, while tRG cells in the cortical VZ are mainly gliogenic, giving rise to the vast majority of cortical astrocytes and oligodendrocytes, and a subpopulation of olfactory bulb interneurons (12, 17). As it turns out, the same limited repertoire of morphogens, such as BMPs, WNTs (Wingless-Int), fibroblast growth factors (FGFs), and Sonic Hedgehog (SHH), are used over and over again across ontogeny and phylogeny, and are involved in all steps of neural development, from neural induction, and telencephalon patterning to neurogenesis and gliogenesis regulation (1, 17–21).

Over the course of evolution, the primate cerebral cortex had a large increase in the number of neurons. Indeed, the human cerebral cortex has the largest number of neurons (16.3 billion) (22, 23), which is a dominant contributor to the “seat” of intelligence and mind, whereas the elephant cerebral cortex, which has twice the mass of the human cerebral cortex, only has 5.6 billion neurons, which is also fewer than ~8 billion neurons in the chimpanzee cerebral cortex (24).

In terms of cortical PyN numbers, there are mainly two determining factors. One is the size of the cortical neuroepithelial and fRG cell pool present in the VZ at the beginning of cortical neurogenesis, which largely determines the PyN number and surface area of the cerebral cortex. This is known as “the radial unit hypothesis” (3, 25). The second is the length of the cortical neurogenic period (2, 26, 27). Indeed, humans have the longest cortical neurogenic period (26), allowing cortical RG cells to produce more PyNs. Human cortical neurogenesis from fRG cells in the VZ extends from GW7 to GW16 (11), and cortical neurogenesis from oRG cells in the OSVZ extends from GW17 to GW26 (12, 17). We found that during mammalian evolution (mouse, ferret, monkey, and human), *bone morphogenic protein 7* (*Bmp7*) is expressed by increasing numbers of cortical RG cells (17). BMP7 in cortical RG cells promotes neurogenesis, inhibits gliogenesis, and thereby extends the neurogenic period, resulting in producing a large number of cortical PyNs. We demonstrate that BMP7 signaling in cortical RG cells inhibits SHH signaling through promoting GLI3 repressor (GLI3R) formation (17). Conversely, SHH signaling in cortical RG cells represses *BMP7* expression, but the molecular mechanisms governing this process remain

Significance

What makes us human? It is our cerebral cortex with the largest number of neurons (16.3 billion) among primates. How to make a large-sized human cerebral cortex? It is the increase in the size of the cortical stem cell pool and the length of the neurogenic period during development. Here, we provide evidence that fibroblast growth factor (FGF)-extracellular signal-regulated kinase (ERK) signaling is elevated in cortical stem cells during development and evolution. We found that ERK signaling promotes the expansion of cortical stem cells and induces *bone morphogenic protein 7* (*Bmp7*) expression, which contributes to the lengthening of the cortical neurogenic period. We propose a model that ERK signaling drives the expansion of the mammalian cortex during evolution.

Author affiliations: ^aState Key Laboratory of Medical Neurobiology and Ministry of Education Frontiers Center for Brain Science, Institutes of Brain Science, and Department of Neurology, Zhongshan Hospital, Fudan University, Shanghai 200032, China

Author contributions: Z.Y. designed research; M.S. and Y.G. performed research; Z.L., L.Y., G.L., Z.X., R.G., and Y.Y. analyzed data; and Z.Y. wrote the paper.

The authors declare no competing interest.

This article is a PNAS Direct Submission. N.S. is a guest editor invited by the Editorial Board.

Copyright © 2024 the Author(s). Published by PNAS. This article is distributed under [Creative Commons Attribution-NonCommercial-NoDerivatives License 4.0 \(CC BY-NC-ND\)](https://creativecommons.org/licenses/by-nc-nd/4.0/).

¹M.S. and Y.G. contributed equally to this work.

²To whom correspondence may be addressed. Email: yangz@fudan.edu.cn.

This article contains supporting information online at <https://www.pnas.org/lookup/suppl/doi:10.1073/pnas.2314802121/-/DCSupplemental>.

Published March 18, 2024.

poorly understood. We also do not know what signals induce *BMP7* expression in cortical RG cells during development and evolution.

In the present study, we report that FGF-extracellular signal-regulated kinase (ERK) signaling promotes cortical RG cell self-renewal and inhibits neural differentiation, which greatly expands the size of the founder population. Furthermore, ERK signaling induces *Bmp7* expression in cortical RG cells, which increases the length of the neurogenic period (17). We demonstrate that ERK signaling and SHH signaling mutually inhibit each other in cortical RG cells. We also provide evidence that ERK signaling is elevated in RG cells during cortical development and evolution. We propose that the expansion of the human cortex may be driven, in part, by the ERK-BMP7-GLI3R signaling pathway in cortical RG cells, which participates in a positive feedback loop through antagonizing SHH signaling. In contrast, during mouse cortical development and evolution, we suggest a model that relatively higher levels of SHH signaling antagonize ERK-BMP7-GLI3R signaling in cortical RG cells, which reduces the size of cortical RG cell pool, represses *Bmp7* expression in dorsal cortical RG cells, and thus reduces the length of the cortical neurogenic period.

Results

Fgf8 Overexpression Promotes the Expansion of Cortical Progenitors and Induces *Bmp7* Expression. Mouse cortical neurogenesis starts to take place following cortical patterning. During early cortical neurogenesis (i.e., E11.0 to E12.5), *Fgf8*, *Fgf17*, *Fgf18*, *Spry1*, and *Spry2* are mainly expressed in the presumptive septum and their expressions extend into the medial cortex (28–30). Interestingly, *Bmp7* is also expressed in the medial cortex (17). Furthermore, previous studies have shown that *Fgf8* and *Bmp7* are coexpressed in the mouse anterior neural ridge (ANR) (31). These observations indicate that *Bmp7* expression might be induced by FGF signaling. To test this hypothesis, we overexpress *Fgf8* using hGFAP-Cre and an inducible *Fgf8* over-expressing allele (*Rosa^{Fgf8}* mice) (SI Appendix, Fig. S1A). The hGFAP-Cre recombinase occurs specifically in cortical RG cells starting at E12.5 resulting in recombined floxed alleles in nearly all cortical RG cells and their progeny from E13.0 (17). Consistent with our hypothesis, strong *Bmp7* expression was observed in the E14.5 neocortical VZ of *hGFAP-Cre; Rosa^{Fgf8}* mice, whereas *Bmp7* expression is restricted in the medial cortex of littermate controls (wild type, WT, or *hGFAP-Cre*) (Fig. 1A). The interaction of FGF8 with FGFRs results in phosphorylation and nuclear translocation of ERK1/2, which phosphorylates target transcription factors (SI Appendix, Fig. S1B). We performed immunohistochemistry experiments using an antibody that detects phosphorylated forms of ERK1/2 (32). At E14.5, pERK⁺ cells in control mice are observed in the cortical VZ and SVZ, whereas we found a greatly enhanced expression of pERK in the cortex of *hGFAP-Cre; Rosa^{Fgf8}* mice (Fig. 1B). We also observed that FGF8 strongly induces SP8 expression (Fig. 1C) (33). Notably, HOPX expression was significantly up-regulated (Fig. 1D). Constitutively overexpression of *Fgf8* also promotes the switch from cortical neurogenesis to gliogenesis, as EGFR and OLIG2 are strongly expressed in cortical VZ and SVZ in a lateral^{high}-medial^{low} gradient (Fig. 1E) (34), whereas their expression was absent in the control cortex at E14.5 (Fig. 1E).

FGF8 regulates cortical patterning by promoting rostral neocortical fates, and repressing caudal neocortical fates, in part through promoting *Etv1*, *Etv4*, *Etv5*, *Mest*, and *Sp8* expression, and repressing *Nr2f1*, *Emx2*, and *Fgfr3* expression (18, 28, 31, 33, 35–39). hGFAP-Cre induction of ectopic *Fgf8* expression occurs about 1 d

after neurogenesis has started and about three days after the early stages in cortical regional patterning. Nonetheless, the ectopic *Fgf8* represses NR2F1 and *Fgfr3* expression in the E14.5 (Fig. 1F and G), consistent with its known function (18, 36, 38). FGF signaling stimulates cell proliferation (40–42). Accordingly, the *hGFAP-Cre; Rosa^{Fgf8}* mice showed an expansion of the cortical VZ (SI Appendix, Fig. S2H).

To obtain unbiased transcriptional information on the effect of the ectopic *Fgf8*, we performed bulk RNA-Seq (SI Appendix, Fig. S1C). We compared gene expression profiles from the cortex of *hGFAP-Cre; Rosa^{Fgf8}* mice and littermate controls at E14.5 and identified more than 4,000 genes that were either up-regulated or down-regulated ($P < 0.05$, Dataset S1). Selected differentially expressed genes are shown in the heat map (Fig. 1H and I), which confirmed our immunostaining and mRNA in situ hybridization results. In addition, FGF signaling response genes *Etv1*, *Etv4*, *Etv5*, *Dusp4*, *Dusp6*, *Fgfr1*, *Spry1*, *Spry2*, and *Spry4* and gliogenesis-related genes *Aldoc*, *Bcan*, *Dio2*, *Fabp7*, and *Tnc* were significantly up-regulated, whereas neurogenesis-related genes *Bcl11a*, *Dmrt3*, *Emx1*, *Eomes* (*Tbr2*), *Neurod1*, *Neurod2*, *Neurod6*, *Neurog1*, and *Neurog2* were down-regulated (Fig. 1H and I).

Taken together, our results reveal that overexpression of *Fgf8* promotes expansion of cortical progenitors and induces *Bmp7* expression in the cortical RG cells. In addition, sustained FGF8 signaling promotes cortical neurogenesis to gliogenesis switch.

Sustained Activation of ERK Signaling Promotes the Expansion of Cortical Progenitors and Induces *Bmp7* Expression. FGF signaling is mediated by the activation of Ras/Raf/Mitogen-activated protein kinase/ERK kinase (MEK)/ERK cascade, phosphatidylinositol-4,5-bisphosphate 3-kinase (PI3K)-AKT, and Phospholipase C Gamma (PLC γ) (SI Appendix, Fig. S1B) (40, 42). ERK signaling can be activated in the *Rosa^{MEK1DD}* mouse, which contains a Cre inducible constitutively active rat *Map2k1* and EGFP alleles. The mutant protein has two serine to aspartic acid substitutions (S218D/S222D) within the catalytic domain (SI Appendix, Fig. S1A).

We first introduced the *hGFAP-Cre* allele into the *Rosa^{MEK1DD}* mice, to study the effect of constitutively active *Map2k1* on intracellular signaling and gene expression. pERK is strongly up-regulated in the cortical VZ and SVZ at E14.5 (Fig. 2A). As expected, activated ERK induced *Bmp7* expression in the cortical VZ (Fig. 2B). Furthermore, HOPX, ETV5, EGFR, and OLIG2 expression was also strongly up-regulated (Fig. 2C–F), whereas NR2F1 and *Fgfr3* expression was down-regulated (Fig. 2G and H). ERK signaling promotes progenitor cell proliferation (43). Accordingly, the VZ length was increased in the cortex of *hGFAP-Cre; Rosa^{MEK1DD}* mice compared with littermate controls (SI Appendix, Fig. S2H).

Bulk RNA-Seq analysis confirmed the above results (Fig. 2I and J and Dataset S2). There were more than 4,000 genes that were either significantly up-regulated or down-regulated in the cortex of E14.5 *hGFAP-Cre; Rosa^{MEK1DD}* mice ($P < 0.05$, Dataset S2). These misregulated genes were related to cell proliferation, survival, growth, metabolism, migration, and differentiation, confirming that ERK signaling regulates these cellular processes in the developing cortex (43). Similar to *Fgf8* overexpression, sustained ERK signaling also promotes *Etv1*, *Etv4*, *Etv5*, *Dusp4*, *Dusp6*, and *Spry2* expression and promotes the onset of cortical gliogenesis (Fig. 2I and J and Dataset S2).

Next, we examined *Nes-Cre; Rosa^{MEK1DD}* (SI Appendix, Fig. S2) and *Emx1-Cre; Rosa^{MEK1DD}* mice (SI Appendix, Fig. S3) and observed similar results to *hGFAP-Cre; Rosa^{MEK1DD}* mice. Because *Nes-Cre* recombination occurs in the neural progenitors around E11.5, both in the pallium and subpallium, we

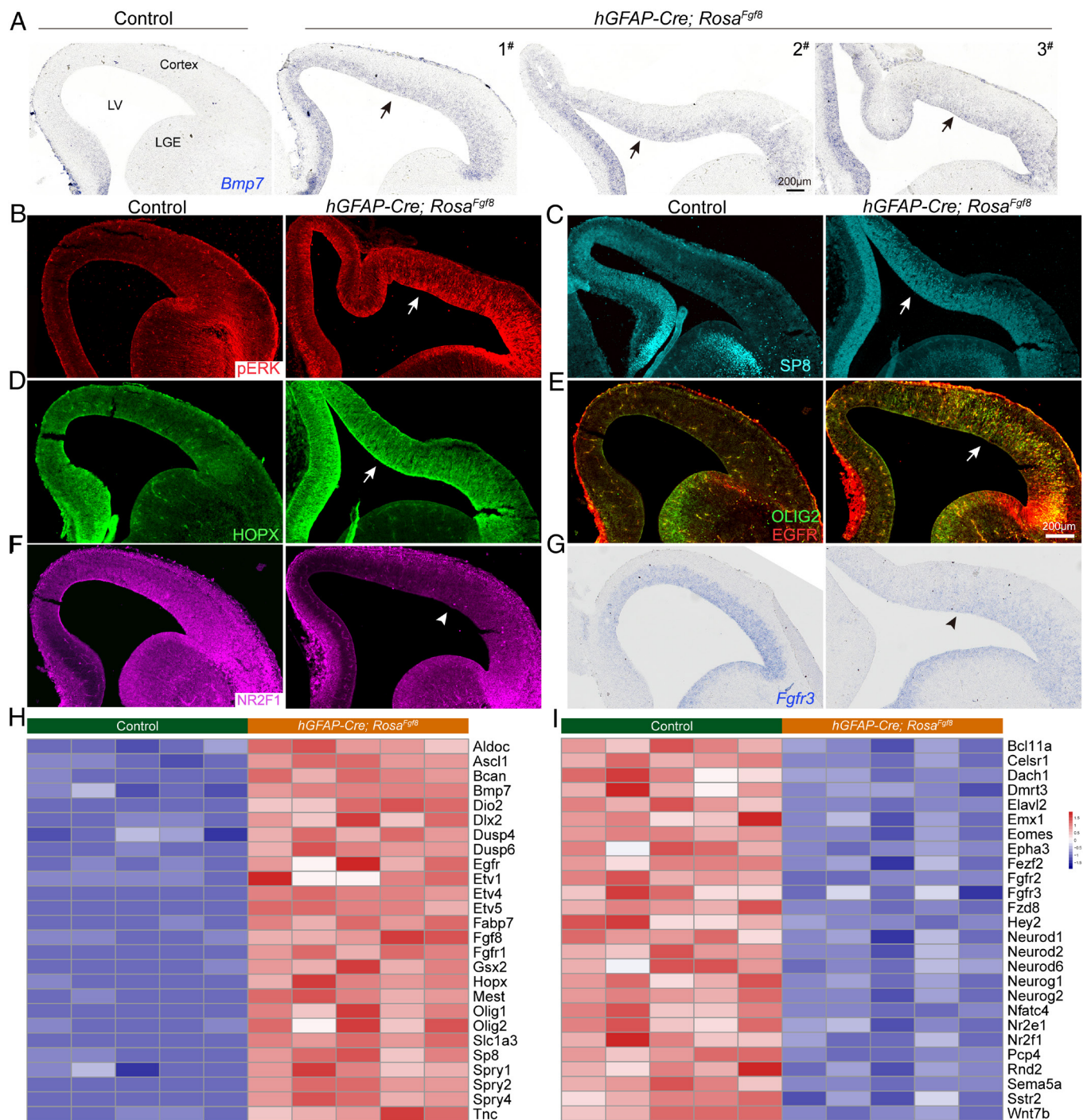


Fig. 1. Overexpression of *Fgf8* expands the cortical progenitor pool and induces *Bmp7* expression in cortical RG cells. (A) mRNA in situ hybridizations on coronal sections through the telencephalon of E14.5 littermate control and *hGFAP-Cre; Rosa^{Fgf8}* mouse embryos (n = 3), showing significant upregulation of *Bmp7* expression in the cortex (arrows). Note that *Bmp7* expression is only detected in the medial cortex of littermate controls. LGE, lateral ganglionic eminence; LV, lateral ventricle. (B–G) Expression of pERK, SP8, HOPX, EGFR, and OLIG2 was greatly increased (arrows), whereas expression of NR2F1 and *Fgfr3* was down-regulated (arrowheads) in the cortex following *Fgf8* overexpression. (H and I) The heat map of bulk RNA-seq data showing expression of neurogenesis genes was down-regulated, whereas expression of FGF8 signaling response genes, *Etv1*, *Etv4*, *Etv5*, *Mest*, *Sp8*, *Spry1*, *Spry2*, and *Spry4* was up-regulated in the *hGFAP-Cre; Rosa^{Fgf8}* cortex (n = 5) compared with littermate controls (n = 5) at E14.5.

found that *Bmp7* expression was also weakly up-regulated in the lateral ganglionic eminence (LGE) at E14.5 (SI Appendix, Fig. S2A). This suggests that ERK signaling inducing *Bmp7* expression in RG cells might be a common rule in certain brain regions, including the neocortex and LGE. In summary, increase in FGF-ERK signaling promotes the expansion of cortical progenitors and induces *Bmp7* expression in cortical RG cells, and

sustained FGF8-ERK activity promotes the switch from the cortical neurogenesis to gliogenesis.

Loss of Cortical ERK Signaling Results in Loss of *Bmp7* Expression, Depletion of Cortical RG Cells, and Premature Neural Differentiation. To further examine the function of ERK signaling in cortical neuroepithelial and RG cells, we conditionally deleted floxed alleles

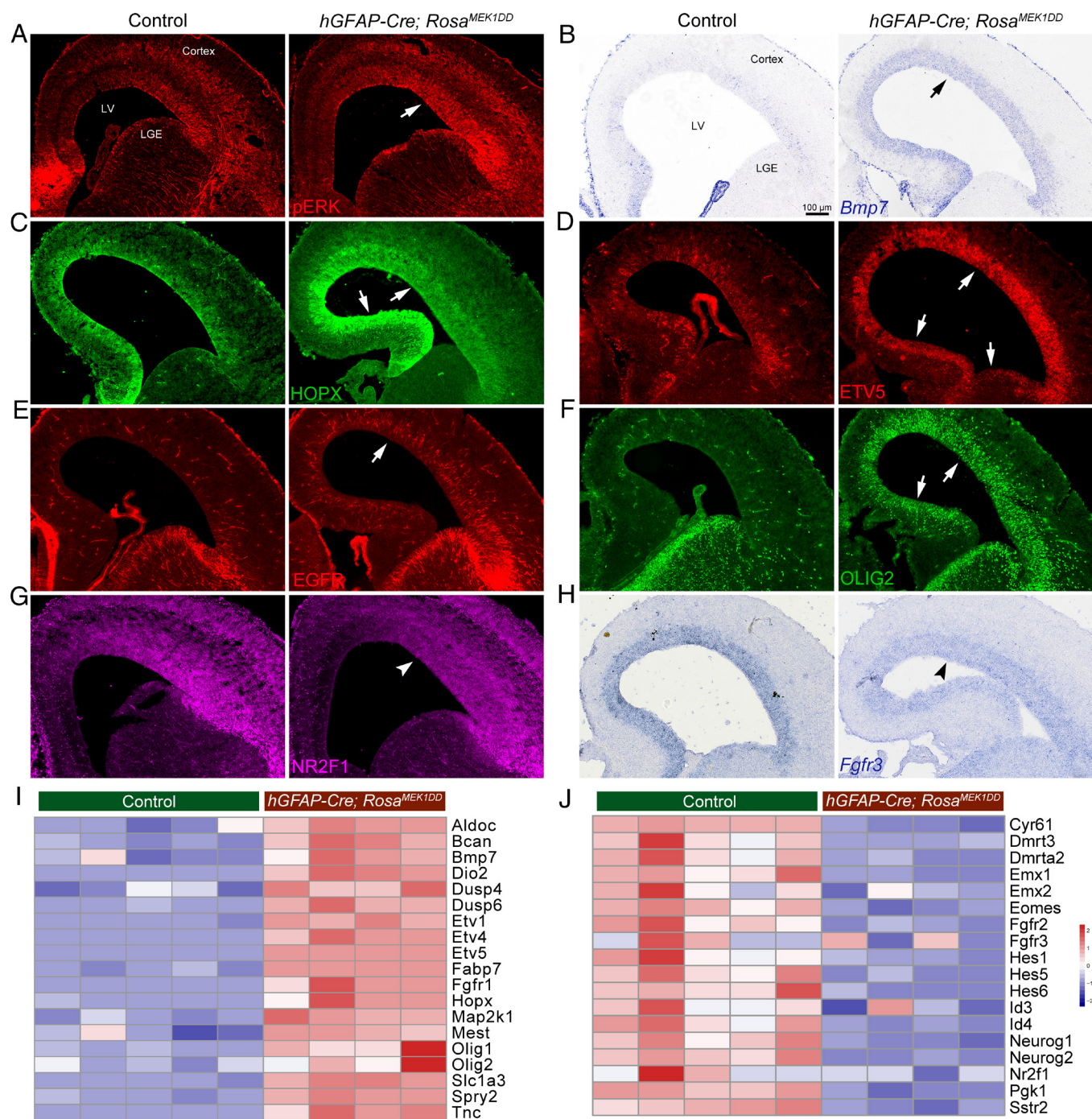


Fig. 2. Constitutive activity of ERK signaling induces *Bmp7* expression in cortical RG cells. (A–F) Expression of pERK, *Bmp7*, HOPX, ETV5, EGFR, and OLIG2 was up-regulated in the cortex of *hGFAP-Cre; Rosa^{MEK1DD}* mice at E14.5 (arrows). (G and H) NR2F1 and *Fgfr3* expression was down-regulated (arrowheads). (I and J) Heat map of selected differentially expressed genes in the E14.5 cortex of *hGFAP-Cre; Rosa^{MEK1DD}* mice (n = 4) relative to controls (n = 5).

of core components of the ERK pathway: *Map2k1* and *Map2k2* (using *Emx1-Cre* line) (SI Appendix, Fig. S1 A and B). We have found that *Map2k1* and *Map2k2* double deletion (*Emx1-Cre; Map2k1/2-dcko*) depleted pERK signal and HOPX expression at E14.5 (Fig. 3 A and B). Loss of ERK signaling also depleted the expression of *Bmp7* in the medial cortex (Fig. 3C). On the other hand, expression of NR2F1 and *Fgfr3* was greatly increased, especially in the medial cortex (Fig. 3 D and E). We observed that a subset of EOMES⁺ PyN IPCs was located at the VZ surface in *Emx1-Cre; Map2k1/2-dcko* mice, while in controls, most EOMES⁺ PyN IPCs were located in the SVZ (Fig. 3F), indicative of precocious production of PyN IPCs. Quantification of the E14.5

cortical VZ length showed a statistically significant decrease of VZ length (SI Appendix, Fig. S2H), suggesting a reduction in the number of cortical RG cells in *Emx1-Cre; Map2k1/2-dcko* mice.

At E17.0, pERK signal and HOPX expression were still completely absent in the cortices of *Emx1-Cre; Map2k1/2-dcko* mice (SI Appendix, Fig. S4 A and B); the thickness of the cortical VZ and SVZ was significantly reduced (SI Appendix, Fig. S4 C–E). Remarkably, the number of cortical PAX6⁺ cells and EOMES⁺ cells was reduced to 50% lower in *Emx1-Cre; Map2k1/2-dcko* mice compared with controls (SI Appendix, Fig. S4 C–G). These observations are consistent with previous results by deletion of all three *Fgf* receptor genes (44, 45) or deletion of both *Mapk1* (*Erk2*) and

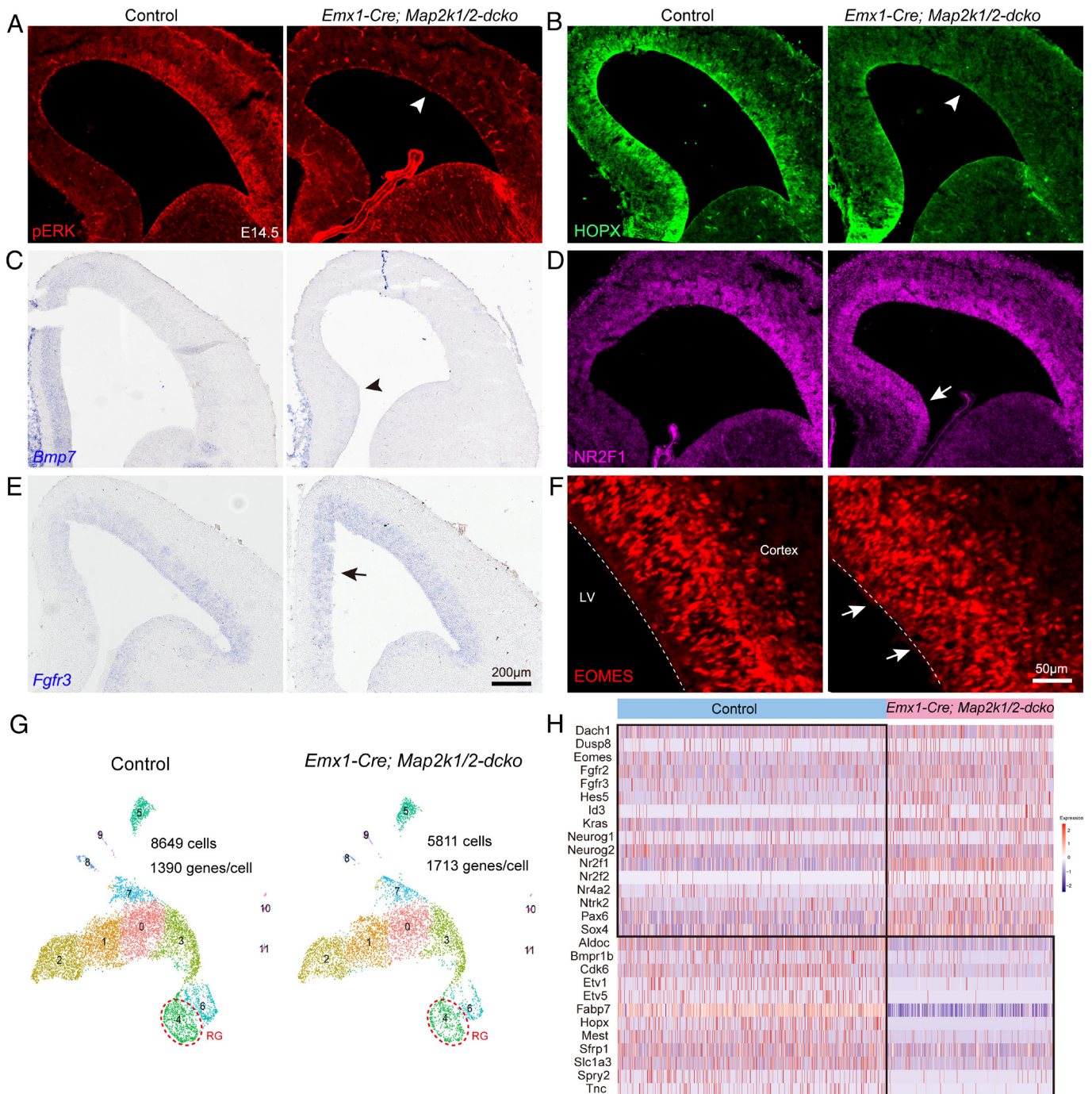


Fig. 3. Deletion of *Map2k1* and *Map2k2* genes in the developing cortex leads to loss of ERK signaling and premature neural differentiation. (A–C) Expression of pERK, HOPX, and *Bmp7* was lost specifically in the cortex of *Emx1-Cre; Map2k1/2-dcko* mice at E14.5 (arrowheads). (D and E) NR2F1 and *Fgfr3* expression was increased in the cortex, especially in the medial cortex (arrows). (F) Immunostaining of EOMES, a marker for PyN IPCs, showing that PyN IPCs located in the VZ surface in *Emx1-Cre; Map2k1/2-dcko* mice at E14.5 (arrows). (G and H) scRNA-Seq analysis and heat map showing expression of selected ERK signaling response genes in cortical RG cells of *Emx1-Cre; Map2k1/2-dcko* mice relative to littermate controls at E14.5. Note that the expression of *Etv1*, *Etv5*, *Hopx*, *Spry2*, and *Tnc* was completely lost in cortical RG cells in *Emx1-Cre; Map2k1/2-dcko* mice.

Mapk3 (*Erk1*) genes (46), indicating that FGF-ERK signaling promotes the self-renewal of cortical RG cell and represses neural differentiation.

scRNA-Seq analysis of the E14.5 cortical cells of *Emx1-Cre; Map2k1/2-dcko* mice and littermate controls confirmed the above results (Fig. 3 G and H and Dataset S3). Without ERK signaling, expression of *Eomes*, *Hes5*, *Neurog1*, *Nr2f1*, and *Nr2f2* in cortical RG cells was up-regulated, indicating premature neural differentiation, whereas expression of ERK response genes *Aldoc*, *Cdk6*, *Fabp7*, and *Slc1a3* was significantly down-regulated, and expression of *Etv1*,

Etv5, *Hopx*, *Mest*, *Spry2*, and *Tnc* in cortical RG cells was nearly completely lost (Fig. 3H).

In summary, our results reveal that ERK signaling is required for maintaining the self-renewal and undifferentiated state of cortical RG cells; ERK signaling is absolutely required for the cortical expression of *Bmp7* and HOPX; and ERK signaling represses cortical expression of NR2F1 and *Fgfr3*. Previously, we have shown that *Bmp7* overexpression in the cortex increases HOPX expression (17), suggesting that both ERK and BMP7 signaling promote HOPX expression.

BMP7-SMAD Signaling Promotes GLI3R Formation. BMP7 binding to the type I and type II BMP receptors on the cell membrane results in the phosphorylation and activation of SMAD1/5/9 proteins, which form a complex with SMAD4 that together regulates gene expression (47). This is the canonical BMP-Smad pathway (47). When *Bmp7* was delivered into the cortical VZ by in utero electroporation (IUE) of *pCAG-Bmp7-Gfp* at E14.5 or E15.5, Western blotting showed increased ratio of GLI3R/GLI3FL (repressor/full-length forms of GLI3) in the E16.5 or E17.5 cortex, mainly due to excess production of GLI3R, which antagonizes SHH signaling (17). Expression of a constitutively active SMO protein that drives SHH signaling (*hGFAP-Cre; Rosa^{SmoM2}* mice) significantly decreased GLI3R expression and increased EGFR expression (17). Here we overexpressed *Bmp7* in the cortical VZ of mice with genetic enhancement in SHH signaling and genetic defect in SMAD signaling (*hGFAP-Cre; Rosa^{SmoM2}* and *hGFAP-Cre; Rosa^{SmoM2}; Smad4^{F/F}* mice) at E15.0 by IUE of *pCAG-Bmp7-Gfp*. Analysis at E17.0 in the *hGFAP-Cre; Rosa^{SmoM2}* mice showed that BMP7 induced increased expression of ID3 and pSMAD1/5/9 and decreased expression of EGFR, *Gli1*, *Ptch1*, and *Gas1* (SI Appendix, Fig. S5 A–H). Importantly, the *Bmp7*-IUE cortex of *hGFAP-Cre; Rosa^{SmoM2}; Smad4^{F/F}* mice showed that none of these gene expression was changed (SI Appendix, Fig. S5 C–H). These results further demonstrate that BMP7 inhibits EGFR expression and promotes GLI3R formation through the canonical SMAD pathway.

SHH-SMO Signaling Antagonizes ERK Signaling in Mouse Cortical RG Cells. In general, SHH signaling (SHH concentration) exhibits in a ventral^{high}-dorsal^{low} and caudal^{high}-rostral^{low} gradient, whereas FGF-ERK signaling exhibits in a rostral^{high}-caudal^{low} gradient during telencephalon patterning and development (20, 48, 49). SHH and FGF8 have a reciprocal regulatory relationship during telencephalon patterning. SHH is required for maintaining *Fgf8* expression (50), and FGF8 is required for *Shh* induction (18). We examined SHH-SMO function in mouse cortical RG cells after neurogenesis has started bypassing the cortical patterning stage. In the E14.5 cortex of *hGFAP-Cre; Rosa^{SmoM2}* mice, the expression of *Gli1*, *Fgf15*, *Fgf3*, NR2F1, EGFR, and OLIG2 was significantly up-regulated, whereas the expression of pERK and HOPX was greatly reduced in RG cells compared with littermate controls (Fig. 4 A–H). These observations were further confirmed by scRNA-Seq analysis (Fig. 4 I and J and Dataset S4), suggesting that SHH-SMO signaling antagonizes ERK signaling in cortical RG cells after the cortical patterning stage, and sustained SHH-SMO activity promotes cortical gliogenesis (51–53).

We next tested whether ERK signaling is increased in cortical RG cells when SHH-SMO function is absent, using *hGFAP-Cre; Smo^{F/F}* mice. At E17.0, expression of pERK, HOPX, and *Bmp7* was up-regulated in the cortical VZ compared to the control mice (SI Appendix, Fig. S6 B–D) (17). FlashTag (CellTrace Yellow) (54) was injected into the lateral ventricle of *Smo^{F/F}* or *hGFAP-Cre; Smo^{F/F}* mice at E17.0. The cortex was collected at E18.0 for cell sorting and scRNA-Seq analysis was performed on FlashTag labeled cells (SI Appendix, Fig. S1D) (17). As anticipated, scRNA-Seq data revealed that expression of *Aldoc*, *Bmp7*, *Dio2*, *Etv1*, *Etv4*, *Etv5*, *Fgfr2*, *Gfap*, *Hopx*, *Nog*, and *Tnc* in cortical RG cells of *hGFAP-Cre; Smo^{F/F}* mice was significantly up-regulated (SI Appendix, Fig. S6I) (17). These results support the idea that, without SHH-SMO function, ERK signaling in cortical RG cells is enhanced.

SHH-SMO signaling inhibits *Bmp7* expression in the mouse cortex (17), most likely due to its antagonizing ERK signaling. To test this further, we reduced FGF-ERK signaling by IUE a soluble

form of *FGFR3c* (*sFGFR3c*) in the E14.0 cortex of *hGFAP-Cre; Smo^{F/F}* mice (SI Appendix, Fig. S6 A and E). *sFGFR3c* is a high-affinity FGF receptor isoform that sequesters endogenous FGF family members, blocking their ability to activate endogenous receptors (35). Both in E17.0 control and *hGFAP-Cre; Smo^{F/F}* mice, the *sFGFR3*-IUE cortex showed decreased expression of pERK and HOPX (SI Appendix, Fig. S6 F and G). Furthermore, *Bmp7* upregulation disappeared upon *sFGFR3c* overexpression (SI Appendix, Fig. S6H), suggesting that an increase in ERK signaling is crucial to induce *Bmp7* expression in the dorsal cortex of *hGFAP-Cre; Smo^{F/F}* mice.

Taken together, our analysis of SHH-SMO gain of function and loss of function phenotypes in mice demonstrates that SHH signaling antagonizes ERK signaling in cortical RG cells after cortical patterning; this then contributes to preventing the spread of *Bmp7* expression from the medial cortex to the dorsal cortex.

Higher Levels of ERK Signaling Activity in Ferret and Human than in Mouse Cortical RG Cells. We recently found that *BMP7* is expressed by increasing numbers of cortical RG cells during mammalian evolution (mouse, ferret, monkey, and human) (17). Because *BMP7* expression in RG cells is dependent on ERK signaling, we suspect that ERK signaling might be also elevated in mammalian cortical RG cells during evolution. We first examined the expression of ERK signaling response genes in cortical fRG cells of the mouse at E15.5 (whole cortex) (55), ferret at E39 (whole cortex) (17), rhesus monkey at E78 (visual cortex) (56), and human at GW14 (prefrontal cortex) (57) by comparative scRNA-Seq analyses (SI Appendix, Fig. S7A) (17) and found that in general, there is an increase in the expression of *BMP7*, *ETV1*, *ETV5*, *FGF2*, *HOPX*, *SLC1A2*, *SLC1A3*, and *SPRY2* in cortical fRG cells during evolution (SI Appendix, Fig. S7 B–D). The most prominent feature is the elevated expression of *SPRY1* in ferret, monkey, and human cortical fRG cells (SI Appendix, Fig. S7D), whereas very few *SPRY1*-expressing fRG cells are in the mouse dorsal cortex (29). The expression of *SPRY* genes is dependent on ERK signaling, and *SPRY* participates in the negative-feedback control of ERK signaling (29, 58). We suspect that because mouse cortical ERK signaling is relatively weak (59), it fails to induce *Spry1* expression in dorsal cortical RG cells.

We next examined the expression of ERK signaling response genes in human cortical fRG and oRG cells (they are both neurogenic) at GW12, GW14, GW18, GW22, GW23, and GW26 by analyzing the published scRNA-Seq dataset (SI Appendix, Fig. S8A) (17, 57, 60). As development proceeds, more cortical RG cells express *ALDOC*, *ACSBG1*, *BMP7*, *DIO2*, *ERG1*, *ETV1*, *FGF1*, *FGF2*, *GFAP*, *FGFR1*, *FGFR2*, *HOPX*, *SLC1A2*, *SLC1A3*, *SPRY1*, and *SPRY2* (SI Appendix, Fig. S8 B–E), indicating an elevation of ERK signaling in human cortical fRG and oRG cells with increasing gestational age.

To validate the above scRNA-Seq analysis results, we performed immunostaining and mRNA in situ hybridization experiments to examine expression of pERK, HOPX, and *BMP7* in the E33 ferret cortex, a developmental time point that is comparable to the E14.5 mouse cortex, as the cortical plate is newly formed in both species at this stage (SI Appendix, Fig. S9 A and B) (61, 62). In the E14.5 mouse cortex, *Bmp7* mRNA was only detected in the medial cortex (SI Appendix, Fig. S9E); pERK and HOPX were mainly expressed in the whole cortical VZ, albeit relatively weak (SI Appendix, Fig. S9 C and D). On the other hand, in the E33 ferret cortex, strong pERK and HOPX expression was seen in cortical fRG cells (SI Appendix, Fig. S9 F and G). Furthermore, *Bmp7* mRNA expression extended much more broadly, from the medial cortex

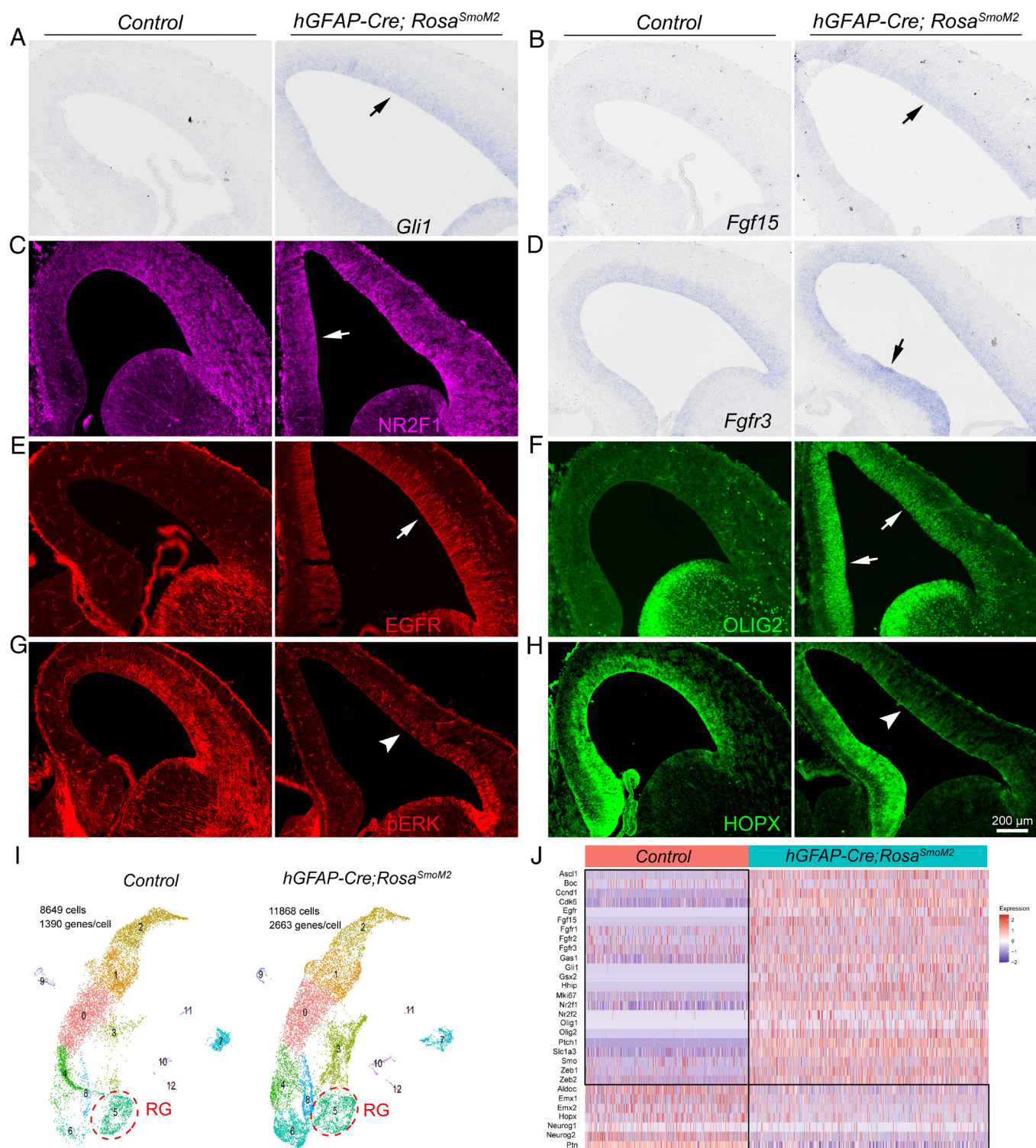


Fig. 4. The SHH-SMO signaling antagonizes ERK signaling in cortical RG cells. (A–H) Expression of *Gli1*, *Fgf15*, NR2F1, *Fgfr3*, EGFR, and OLIG2 was greatly up-regulated (arrows), whereas expression of pERK and HOPX was severely reduced (arrowheads) in the cortex of *hGFAP-Cre; Rosa^{SmoM2}* mice compared with littermate controls at E14.5. (I and J) scRNA-Seq analysis and heat map showing expression of key signature genes in cortical RG cells of *hGFAP-Cre; Rosa^{SmoM2}* mice relative to controls at E14.5.

to the dorsolateral cortex (*SI Appendix, Fig. S9H*), providing evidence that relatively stronger ERK signaling is present in the ferret cortical VZ than that in the mouse cortical VZ.

We also examined pERK and HOPX expression patterns in GW18 human cortical sections; these high-quality brain sections were used in our previous studies (12, 17, 63, 64). scRNA-Seq analysis of the GW18 human cortex from published datasets (60), clearly

revealed that human cortical oRG cells are neurogenic, while tRG cells are gliogenic (17), and ERK signaling response genes *ACSBG1*, *BMP7*, *ETV1*, *ETV5*, *FGFR1*, *GFAP*, *HOPX*, *SI00B*, *SLCIA2*, *SLCIA3*, *SPRY1*, *SPRY2*, and *TNC* are highly expressed in oRG cells than that in tRG cells (*SI Appendix, Fig. S10 A–C* and *Dataset S5*). Consistent with this bioinformatic analysis, we observed stronger pERK immunoreactivity in the soma and radial fibers of

oRG cells in the OSVZ compared with tRG cells in the cortical VZ (Fig. 5 *A–D*), and most HOPX⁺ RG cells were coexpressed with pERK (Fig. 5 *C* and *D*). We propose that similar to the mouse cortex, cortical expression of *BMP7* and HOPX in other mammals, including humans, is also induced by ERK signaling.

Taken together, by integrating analyses of published mouse, ferret, monkey, and human cortical scRNA-Seq datasets with our immunostaining and mRNA in situ hybridization experiments, we provide strong evidence that ERK signaling is elevated in ferret and human cortical RG cells compared with mouse cortical RG cells.

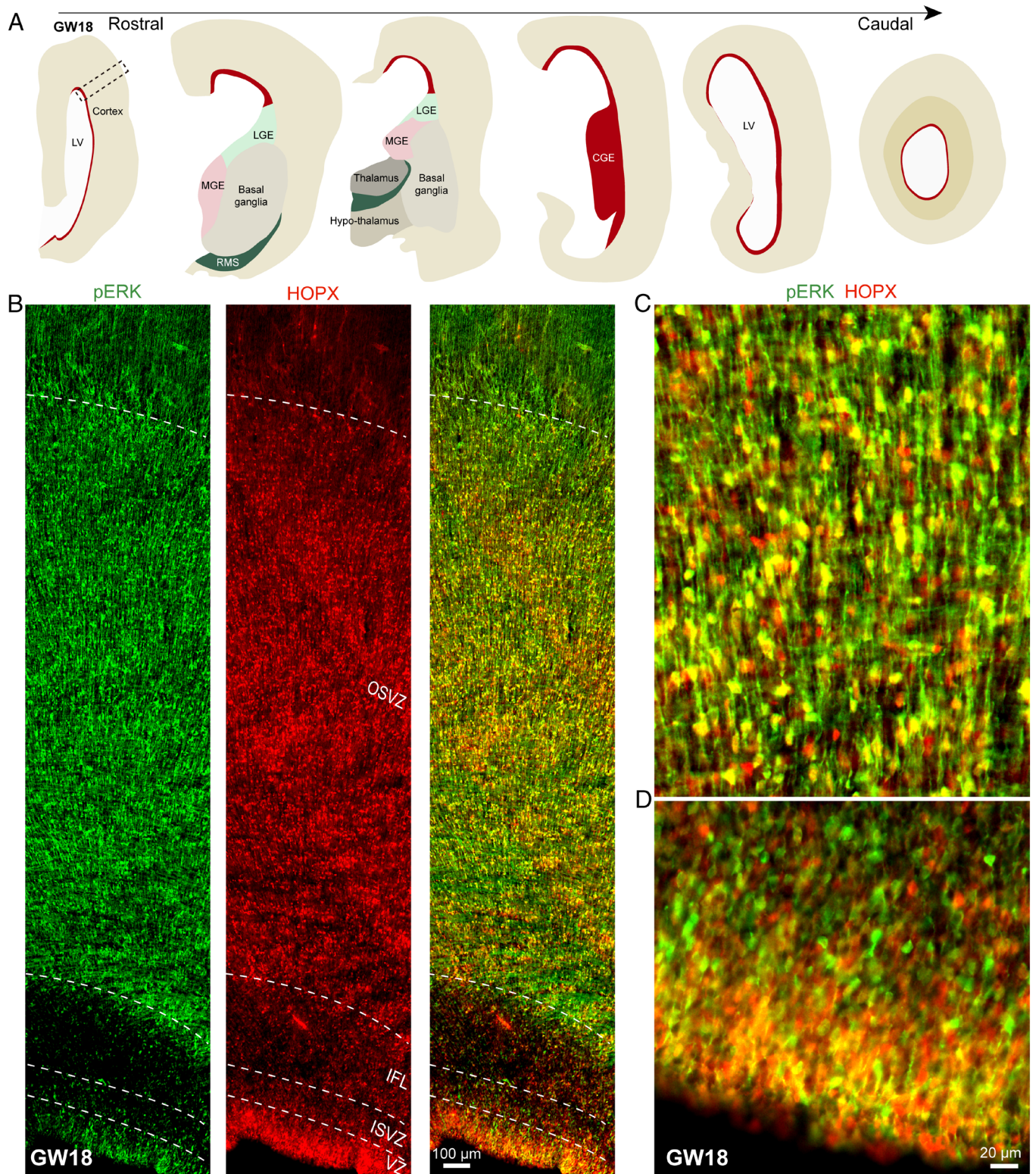


Fig. 5. Stronger ERK signaling activity in human cortical oRG cells than in tRG cells. (A) The diagram showing brain sections spanning the rostral-caudal extent of the human telencephalon at GW18. CGE, caudal ganglionic eminence; MGE, medial ganglionic eminence; RMS, rostral migratory stream. (B) The coronal section through the rostral telencephalon (the outlined area in A) at GW18 double immunostained with pERK and HOPX. ISVZ, inner subventricular zone, IFL, inner fiber layer. (C and D) Higher magnification images showing that pERK and HOPX immunoreactivity is stronger in the cortical OSVZ (C) than cortical VZ (D).

Discussion

There are 5 main findings in this study. 1) FGF-ERK signaling promotes the self-renewal and expansion of cortical neuroepithelial and RG cells, which increases the size of the cortical neural stem cell pool. 2) FGF-ERK signaling induces *Bmp7* expression in cortical RG cells, which increases the length of the neurogenic period. 3) BMP7-SMAD signaling promotes GLI3R formation, which inhibits SHH signaling. 4) SHH signaling antagonizes ERK-BMP7 signaling in cortical RG cells, which promotes cortical cell proliferation and gliogenesis. 5) ERK signaling is elevated in ferret and human cortical RG cells compared with mouse cortical RG cells. Therefore, ERK-BMP7-GLI3R and SHH signaling, which mutually inhibit each other, coordinately regulate cortical development. On the basis of these results, we wish to suggest a principle of mammalian cortical development, expansion, and evolution (Fig. 6 and *SI Appendix*, Fig. S11).

ERK Signaling Expands Mammalian Cortical RG Cells and Increases the Neurogenic Period. In this study, we believe that we have identified a core mechanism that drives cortical expansion and evolution; we propose that FGF-ERK signaling drives evolutionary expansion of the mammalian cerebral cortex (Fig. 6 *A–C* and *SI Appendix*, Fig. S11). This conserved mechanism has an origin dating back at least 500 million years, as the anterior neural ridge (ANR)-like genetic regulatory program of FGF signaling is present in the hemichordate and amphioxus (65). The ANR in the mouse expresses *Fgf8* and *Bmp7* (31). Furthermore, the ANR-derived rostral telencephalic patterning center (RPC) produces FGFs (FGF8/17/18) (19, 28, 30, 31, 35), and when FGFs initiate cortical patterning, the neocortical primordium is roughly the same size in the mouse, ferret and human (62), indicating that molecular mechanisms (e.g., FGF signaling) that pattern the mouse neocortex are conserved across mammalian species (*SI Appendix*, Fig. S11), which is supported by recent scRNA-Seq and spatial transcriptomics analysis of the neocortical primordium of the rhesus macaque (66) and human (67).

After neural tube closure, the dorsal and ventral telencephalon give rise to pallial (cortical and hippocampal) and subpallial structures, respectively. We propose that FGF-ERK signaling continually plays a crucial role in driving mammalian cortical expansion during evolution (Fig. 6 and *SI Appendix*, Fig. S11). The most recent ancestor to all mammals, i.e., 100 Mya, is assumed to have already been in some degree gyrencephalic (26, 68) and is assumed to have a subset of fRG cells in the developing dorsal cortex that express relatively higher levels of pERK. Elevated ERK signaling in cortical fRG cells induces *BMP7* expression, which promotes GLI3R production and represses SHH signaling (17). A decrease in SHH signaling in cortical fRG cells further enhances ERK signaling. Therefore, ERK-BMP7-GLI3R signaling in cortical fRG cells participates in a positive feedback loop (Fig. 6*B*), which increases the size of cortical RG cell pool, restrains but allows neurogenesis, while inhibiting gliogenesis, and thus increases the length of the neurogenic period. In the human developing cortex, this ERK-BMP7-GLI3R positive feedback in fRG cells most likely starts at the beginning of neurogenesis (GW7) and ends at the beginning of gliogenesis (GW16). We hypothesize that SHH concentration in cerebrospinal fluid (CSF) is reduced in the enlarged lateral ventricle of big-brained mammals during cortical development and evolution, which could contribute to a further decrease in SHH signaling and an increase ERK-BMP7-GLI3R signaling in cortical fRG cells (*SI Appendix*, Fig. S11).

In the absence of SHH signaling, GLI3FL (GLI3 activator) protein is processed to GLI3R that represses SHH signaling. This process depends on adenylyl cyclase-mediated cAMP-dependent

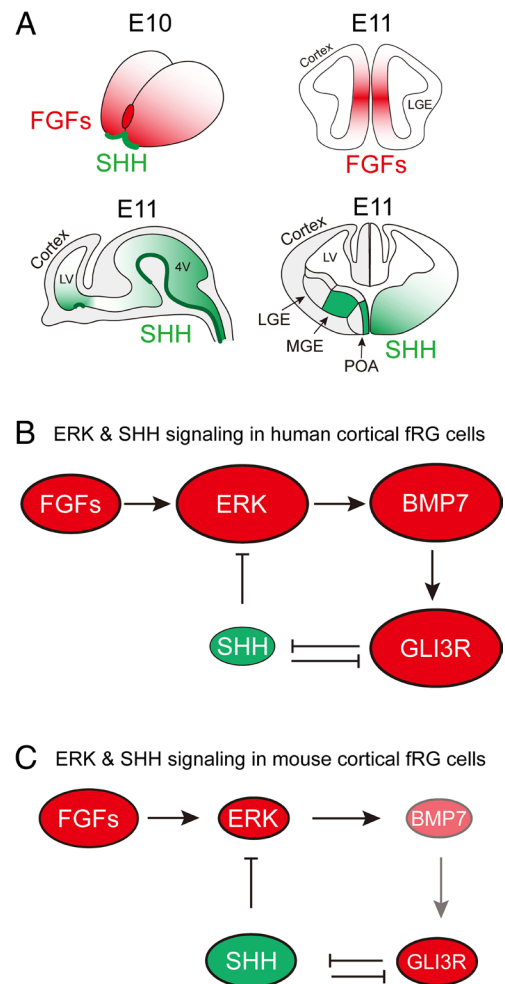


Fig. 6. The proposed principle of human and mouse cortical development and evolution. (A) During mouse early telencephalon patterning and development, FGFs are expressed in the rostral patterning center, whereas SHH is expressed in the POA and MGE-derived neurons. In general, FGF-ERK signaling exhibits in a rostral^{high}-caudal^{low} gradient, whereas SHH-SMO signaling exhibits in a ventral^{high}-dorsal^{low} and caudal^{high}-rostral^{low} gradient. 4V, fourth ventricle; POA, preoptic area. (B) We propose that ERK signaling drives the expansion and evolution of the human cortex. At the beginning of cortical neurogenesis in the most recent ancestor to all mammals, it is assumed that there is already a subset of cortical fRG cells that express relatively higher levels of pERK. Elevated ERK signaling in these cortical fRG cells promotes *BMP7* expression, which increases GLI3R generation and represses SHH signaling. A decrease in SHH signaling in cortical fRG cells further enhances ERK signaling. Therefore, the ERK-BMP7-GLI3R signaling pathway in cortical fRG cells participates in a positive feedback loop, which expands the cortical fRG cell pool, increases the length of the cortical neurogenic period, and thus drives cortical development, expansion, and evolution. (C) We propose that SHH signaling may drive mouse cortical evolutionary dwarfism. During mouse cortical development and evolution, smaller brains with the smaller lateral ventricle results in relatively higher levels of SHH signaling in the cortex, which antagonizes ERK signaling. Relatively weak ERK signaling fails to induce *Bmp7* expression in the dorsal cortical RG cells. Therefore, mouse cortical neurogenesis is mainly protected by GLI3R, but not BMP7, resulting in a shortened period of cortical neurogenesis (for example, from more than 130 d in humans to about 7 d in mice), which is associated with a greatly reduced number of cortical neurons and cortical size.

protein kinase A (PKA) (69, 70). Around midterm gestation, human cortical fRG cells have CXCL12 and CXCR4 expression (12, 17), whereas mouse cortical RG cells express extremely low levels of CXCL12 and CXCR4 (71). CXCR4 is a GPCR that activates G α i protein and inhibits cAMP-PKA signaling. Thus, activation of CXCL12/CXCR4 in human fRG cells decreases GLI3R production (72), increases GLI3FL production, and enhances SHH signaling, thereby interrupting the ERK-BMP7-GLI3R positive

feedback loop in cortical fRG cells. Previous studies have shown that CXCL12/CXCR4 also activates PI3K/AKT/mTOR and YAP-CCN1/2 signaling (73, 74). We propose that SHH signaling (including CXCL12/CXCR4 signaling) combined with ERK signaling are the major forces that drive human cortical *BMP7*-expressing fRG cells to give rise to tRG and oRG cells around GW16 (17), and ERK-BMP7-GLI3R signaling is crucial for generating and maintaining the self-renewing oRG stem cell identity in the OSVZ, although this hypothesis is under investigation.

tRG cells are believed to inherit the apical domain from fRG cells, and primary cilia of tRG cells contact the CSF in the lateral ventricle, receiving CSF SHH molecules (51, 75, 76). tRG cells also express higher levels of CXCL12/CXCR4 (17), which results in expressing higher levels of GLI3FL, and lower levels of GLI3R and *BMP7*. This promotes EGFR expression in tRG cells, as GLI3R and *BMP7* inhibit EGFR expression (17). The onset of EGFR expression in tRG cells is a strong signal for the neurogenesis-to-gliogenesis switch (12, 17, 34, 77, 78). In contrast, oRG cells do not express CXCL12, but express CXCL14 and CXCR4 (17), and CXCL14/CXCR4 likely exerts an inhibitory effect on the CXCL12/CXCR4 signaling pathway (79). Therefore, ERK-BMP7-GLI3R expression in oRG cells in the cortical OSVZ continues to participate in a positive feedback loop, which makes oRG cells neurogenic from GW17 to at least GW26, continually producing upper layer PyNs (12, 17). The oRG cells do not express EGFR and do not give rise to OPCs or interneurons (12, 17). On the other hand, EGFR-expressing primed tRG cells in the cortical VZ are mainly gliogenic, generating basal multipotent intermediate progenitor cells (bMIPCs) that express EGFR, ASCL1, and OLIG2/1 (12). bMIPCs then undergo several rounds of mitosis and generate most of the cortical oligodendrocytes, astrocytes, and a subpopulation of olfactory bulb interneurons (12, 34). This two-germinal-zone system in the human developing cortex ensures that the onset of tRG gliogenesis normally occurs in the VZ, as glial cells have multiple indispensable functions in the developing cortex (80), while oRGs in the OSVZ continue to produce neurons (12, 17), which significantly increases the length of the neurogenic period, a process that is critical for producing the largest number of cortical PyNs among primates (2, 26, 27).

SHH Signaling may Contribute to the Shortening of the Mouse Cortical Neurogenic Period. The lissencephalic mouse is believed to have originated from a larger and gyrencephalic ancestor (26, 68). This is known as evolutionary dwarfism (phyletic dwarfism), a process in which large animals tend to evolve smaller bodies, followed by the simplification of cortical gyrification with a relatively smaller brain (68). Smaller brains with the smaller lateral ventricle may result in higher concentrations of SHH that bath the cortical VZ, and which antagonizes ERK signaling during development and evolution (Fig. 6C). Although ERK signaling is gradually elevated in parts of the mouse cortical progenitor domains (29, 37), it still fails to induce *Bmp7* expression in the dorsal cortical fRG cells. However, when cortical SHH-SMO signaling is blocked in *hGFAP-Cre; Smo^{Fl/F}* mice, elevated ERK signaling is able to induce *Bmp7* expression in a subset of cortical fRG cells (17). Therefore, during mouse cortical development, *Bmp7* expression is restricted to the medial cortex (17), in which FGF8/17/18-ERK signaling is stronger than the dorsal cortex (28, 29, 37). Thus, mouse cortical neurogenesis is mainly protected by GLI3R, but not *BMP7*. Relatively lower ERK signaling reduces the size of cortical RG cell pool and also shortens the neurogenic period as lack of *BMP7* protection. After only 7 d of neurogenesis, around E17.0, mouse cortical gliogenesis starts from the lateral cortex and spreads to the medial cortex (34), whereas human cortical RG cells generate PyNs for 130 d (17). This is likely the main reason that the mouse cortex only has ~13.7 million

neurons, whereas the human cortex has ~16.3 billion neurons (22–24).

Multiple Types of Genetic Evidence Support Our Proposed Principle of Cortical Expansion and Evolution. First, the normal development and expansion of the human cortex provide the strongest evidence supporting our proposal that it is ERK signaling that drives evolutionary expansion of the mammalian cerebral cortex. The human frontal cortex, the center of complex thinking, planning, and decision-making, is the most highly developed and expanded brain structure in mammal evolution (4, 25). FGFs, released at the rostral patterning center and followed by subsequent diffusion, generate a rostral^{high}-caudal^{low} gradient of FGF-ERK signaling in the cortex. This is thought to control the size of the rostral telencephalon (1, 18, 20, 28, 35, 49, 81). Here, we identified that ERK-BMP7 signaling plays a crucial role in expanding the size of the RG cell pool and increasing the length of the neurogenic period (17). Furthermore, ERK-BMP7 signaling is elevated during cortical development and evolution; this results in significant expansion of the human cortex, especially the frontal lobe.

Second, the abnormal development and expansion of the human temporal and occipital cortex in Thanatophoric Dysplasia (TD) patients provide another strong genetic evidence that supports our principle. TD is a lethal form of short-limbed dwarfism caused by abnormal mutations of the *FGFR3*, which lead to constitutive activation of *FGFR3* tyrosine kinase activity (41, 82, 83). *FGFR3* gain of function mutation in TD patients significantly strengthens ERK signaling (84, 85), which may further enhance *BMP7* expression. *FGFR3* is expressed in a high caudomedial-low rostrolateral gradient in the human (86), ferret (87) and mouse cortical neuroepithelial and RG cells (36, 38). Therefore, constitutive activation of the mutant *FGFR3* protein (independent of the ligand of FGFs), may induce the higher level of ERK-BMP7 signaling in the caudal cortex, causing the significant expansion of temporal and occipital lobe in TD patients (41, 83). We propose that mutant *FGFR3* may also enhance ERK-BMP7 signaling in chondrocytes that antagonizes Indian Hedgehog signaling through promoting GLI3R formation, which inhibits their proliferation, enhances differentiation, promotes bone formation and fusion of ossification centers, resulting in skeletal dwarfism. Notably, the TD mouse provides an excellent model for the human TD, as they also exhibit severe dwarfism, perinatal lethality, and the expansion of the cortex (41, 82, 83), further indicating that FGF-ERK signaling supports cortical expansion.

Finally, because *BMP* signaling also functions to maintain stem cells in a quiescent state, we suggest that *BMP7*- and *GLI3R*-expressing RG cells in the mouse medial cortex (similar to human cortical fRG and oRG cells), when they receive strong cell proliferation signals, are able to sustain their self-renewal, maintain neurogenesis, and inhibit gliogenesis for a longer time than that of lateral cortical RG cells (17). Therefore, abnormal cortical folding is always observed in the medial cortex in those transgenic mouse models for studying cortical expansion, including *hGFAP-Cre; Rosa^{SmoM2}* (88), *Emx1-Cre; Gli3^{Fl/F}* (89), *Emx1-Cre; Cep83^{Fl/F}* (90), and *hGFAP-Cre; Pik3ca^{H1047R}* (conditional activating mutations of *Pik3ca*) (91) mouse lines, further highlighting that ERK-BMP7-GLI3R signaling plays a similar role in driving mouse cortical development and evolution.

Materials and Methods

All procedures and animal care followed the Fudan University guidelines. Histology, transgenic assays, plasmid construction, IUE, mouse and ferret mRNA in situ hybridization, bulk RNA-Seq analysis, scRNA-Seq analysis, microscopy and imaging, and quantification and statistical analysis were performed and analyzed

according to published protocols. More details regarding specific experimental procedures and analyses can be found in *SI Appendix*.

Data, Materials, and Software Availability. scRNA-Seq data of the E14.5 cortex of control mice (*Map2k1* and *Map2k2* flox), E14.5 cortex of *Emx1-Cre*; *Map2k1/2-dcko* mice, and E14.5 cortex of *hGFAP-Cre*; *Rosa^{SmoM2}* mice and bulk RNA-Seq data of the E14.5 cortex of control mice ($n = 5$), E14.5 cortex of *hGFAP-Cre*; *Rosa^{Fgf8}* mice ($n = 5$), and E14.5 cortex of *hGFAP-Cre*; *Rosa^{MEK1DD}* mice ($n = 4$) used in this study have been deposited in the Gene Expression Omnibus (GEO) under accession number [GSE240381](https://www.ncbi.nlm.nih.gov/geo/query/acc.cgi?acc=GSE240381). The E18.0 *Smo^{Fl/Fl}* (control) and *hGFAP-Cre*; *Smo^{Fl/Fl}* mouse cortex and E39 ferret cortex scRNA-seq data were

used in previous studies (17) ([GSE221389](https://doi.org/10.1073/pnas.2314802121)). All other data are included in the manuscript and/or [supporting information](#).

ACKNOWLEDGMENTS. We are grateful to Prof. Yanding Zhang at Fujian Normal University for sharing the *Rosa^{Fgf8}* mouse. This study was supported by the Ministry of Science and Technology of China (STI2030-2021ZD0202300), National Natural Science Foundation of China (NSFC 31820103006, 32070971, 32100768, 32200776, and 32200792), Shanghai Municipal Science and Technology Major Project (No. 2018SHZDX01), ZJ Lab, and Shanghai Center for Brain Science and Brain-Inspired Technology.

1. M. Sur, J. L. Rubenstein, Patterning and plasticity of the cerebral cortex. *Science* **310**, 805–810 (2005).
2. B. K. Stepien, S. Vaid, W. B. Huttner, Length of the neurogenic period—A key determinant for the generation of upper-layer neurons during neocortex development and evolution. *Front. Cell Dev. Biol.* **9**, 676911 (2021).
3. P. Rakic, Specification of cerebral cortical areas. *Science* **241**, 170–176 (1988).
4. Z. Molnar *et al.*, New insights into the development of the human cerebral cortex. *J. Anat.* **235**, 432–451 (2019).
5. J. H. Lui, D. V. Hansen, A. R. Kriegstein, Development and evolution of the human neocortex. *Cell* **146**, 18–36 (2011).
6. A. M. M. Sousa, K. A. Meyer, G. Santpere, F. O. Gulden, N. Sestan, Evolution of the human nervous system function, structure, and development. *Cell* **170**, 226–247 (2017).
7. Y. Lin *et al.*, Behavior and lineage progression of neural progenitors in the mammalian cortex. *Curr. Opin. Neurobiol.* **66**, 144–157 (2021).
8. A. Kriegstein, A. Alvarez-Buylla, The glial nature of embryonic and adult neural stem cells. *Annu. Rev. Neurosci.* **32**, 149–184 (2009).
9. A. A. Pollen *et al.*, Molecular identity of human outer radial glia during cortical development. *Cell* **163**, 55–67 (2015).
10. S. C. Noctor, A. C. Flint, T. A. Weissman, R. S. Dammerman, A. R. Kriegstein, Neurons derived from radial glial cells establish radial units in neocortex. *Nature* **409**, 714–720 (2001).
11. T. J. Nowakowski, A. A. Pollen, C. Sandoval-Espinosa, A. R. Kriegstein, Transformation of the radial glia scaffold demarcates two stages of human cerebral cortex development. *Neuron* **91**, 1219–1227 (2016).
12. L. Yang, Z. Li, G. Liu, X. Li, Z. Yang, Developmental origins of human cortical oligodendrocytes and astrocytes. *Neurosci. Bull.* **38**, 47–68 (2022).
13. I. Reillo, C. de Juan Romero, M. A. Garcia-Cabezas, V. Borrell, A role for intermediate radial glia in the tangential expansion of the mammalian cerebral cortex. *Cereb. Cortex* **21**, 1674–1694 (2011).
14. D. V. Hansen, J. H. Lui, P. R. Parker, A. R. Kriegstein, Neurogenic radial glia in the outer subventricular zone of human neocortex. *Nature* **464**, 554–561 (2010).
15. S. A. Fietz *et al.*, OSVZ progenitors of human and ferret neocortex are epithelial-like and expand by integrin signaling. *Nat. Neurosci.* **13**, 690–699 (2010).
16. B. E. LaMonica, J. H. Lui, D. V. Hansen, A. R. Kriegstein, Mitotic spindle orientation predicts outer radial glial cell generation in human neocortex. *Nat. Commun.* **4**, 1665 (2013).
17. Z. Li *et al.*, BMP7 expression in mammalian cortical radial glial cells increases the length of the neurogenic period. *Protein Cell* **15**, 21–35 (2024).
18. E. E. Storm *et al.*, Dose-dependent functions of *Fgf8* in regulating telencephalic patterning centers. *Development* **133**, 1831–1844 (2006).
19. R. V. Hoch, J. A. Clarke, J. L. Rubenstein, *Fgf* signaling controls the telencephalic distribution of Fgf-expressing progenitors generated in the rostral patterning center. *Neural. Dev.* **10**, 8 (2015).
20. J. M. Hebert, G. Fishell, The genetics of early telencephalon patterning: Some assembly required. *Nat. Rev. Neurosci.* **9**, 678–685 (2008).
21. E. A. Grove, T. Fukuchi-Shimogori, Generating the cerebral cortical area map. *Annu. Rev. Neurosci.* **26**, 355–380 (2003).
22. F. A. Azevedo *et al.*, Equal numbers of neuronal and nonneuronal cells make the human brain an isometrically scaled-up primate brain. *J. Comp. Neurol.* **513**, 532–541 (2009).
23. S. Herculano-Houzel, K. Catania, P. R. Manger, J. H. Kaas, Mammalian brains are made of these: A dataset of the numbers and densities of neuronal and nonneuronal cells in the brain of glires, primates, scandentia, eulipotyphlans, afrotherians and artiodactyls, and their relationship with body mass. *Brain Behav. Evol.* **86**, 145–163 (2015).
24. S. Herculano-Houzel *et al.*, The elephant brain in numbers. *Front. Neuroanat.* **8**, 46 (2014).
25. P. Rakic, A century of progress in corticogenesis: From silver impregnation to genetic engineering. *Cereb. Cortex* **16**, i3–17 (2006).
26. E. Lewitus, I. Kelava, A. T. Kalinka, P. Tomancak, W. B. Huttner, An adaptive threshold in mammalian neocortical evolution. *PLoS Biol.* **12**, e1002000 (2014).
27. N. Picco, F. Garcia-Moreno, P. K. Maini, T. E. Woolley, Z. Molnar, Mathematical modeling of cortical neurogenesis reveals that the founder population does not necessarily scale with neurogenic output. *Cereb. Cortex* **28**, 2540–2550 (2018).
28. J. A. Cholfin, J. L. Rubenstein, Frontal cortex subdivision patterning is coordinately regulated by *Fgf8*, *Fgf17*, and *Emx2*. *J. Comp. Neurol.* **509**, 144–155 (2008).
29. A. Faedo, U. Borello, J. L. Rubenstein, Repression of *Fgf* signaling by sprouty1–2 regulates cortical patterning in two distinct regions and times. *J. Neurosci.* **30**, 4015–4023 (2010).
30. U. Borello *et al.*, *FGF15* promotes neurogenesis and opposes *FGF8* function during neocortical development. *Neural. Dev.* **3**, 17 (2008).
31. K. Shimamura, J. L. Rubenstein, Inductive interactions direct early regionalization of the mouse forebrain. *Development* **124**, 2709–2718 (1997).
32. L. B. Corson, Y. Yamanaka, K. M. Lai, J. Rossant, Spatial and temporal patterns of ERK signaling during mouse embryogenesis. *Development* **130**, 4527–4537 (2003).
33. S. Sahara, Y. Kawakami, J. C. Izpisua Belmonte, D. D. O’Leary, Sp8 exhibits reciprocal induction with *Fgf8* but has an opposing effect on anterior-posterior cortical area patterning. *Neural. Dev.* **2**, 10 (2007).
34. X. Li *et al.*, Decoding cortical glial cell development. *Neurosci. Bull.* **37**, 440–460 (2021).
35. T. Fukuchi-Shimogori, E. A. Grove, Neocortex patterning by the secreted signaling molecule *FGF8*. *Science* **294**, 1071–1074 (2001).
36. S. Garell, K. J. Huffman, J. L. Rubenstein, Molecular regionalization of the neocortex is disrupted in *Fgf8* hypomorphic mutants. *Development* **130**, 1903–1914 (2003).
37. H. Hasegawa *et al.*, Lamina patterning in the developing neocortex by temporally coordinated fibroblast growth factor signaling. *J. Neurosci.* **24**, 8711–8719 (2004).
38. T. Fukuchi-Shimogori, E. A. Grove, *Emx2* patterns the neocortex by regulating *FGF* positional signaling. *Nat. Neurosci.* **6**, 825–831 (2003).
39. G. Caronia-Brown, M. Yoshida, F. Gulden, S. Assimakopoulos, E. A. Grove, The cortical hem regulates the size and patterning of neocortex. *Development* **141**, 2855–2865 (2014).
40. F. Guillemot, C. Zimmer, From cradle to grave: The multiple roles of fibroblast growth factors in neural development. *Neuron* **71**, 574–588 (2011).
41. T. Iwata, R. F. Hevner, Fibroblast growth factor signaling in development of the cerebral cortex. *Dev. Growth Differ.* **51**, 299–323 (2009).
42. I. Mason, Initiation to end point: The multiple roles of fibroblast growth factors in neural development. *Nat. Rev. Neurosci.* **8**, 583–596 (2007).
43. H. Lavoie, J. Gagnon, M. Therrien, ERK signalling: A master regulator of cell behaviour, life and fate. *Nat. Rev. Mol. Cell Biol.* **21**, 607–632 (2020).
44. W. Kang, L. C. Wong, S. H. Shi, J. M. Hebert, The transition from radial glial to intermediate progenitor cell is inhibited by *FGF* signaling during corticogenesis. *J. Neurosci.* **29**, 14571–14580 (2009).
45. B. G. Rash, H. D. Lim, J. J. Breunig, F. M. Vaccarino, *FGF* signaling expands embryonic cortical surface area by regulating Notch-dependent neurogenesis. *J. Neurosci.* **31**, 15604–15617 (2011).
46. O. Imamura, G. Pages, J. Pouyssegur, S. Endo, K. Takishima, ERK1 and ERK2 are required for radial glial maintenance and cortical lamination. *Genes Cells* **15**, 1072–1088 (2010).
47. R. N. Wang *et al.*, Bone Morphogenetic Protein (BMP) signaling in development and human diseases. *Genes Dis.* **1**, 87–105 (2014).
48. S. Douceau, T. Deutsch Guerrero, J. Ferent, Establishing hedgehog gradients during neural development. *Cells* **12**, 225 (2023).
49. R. V. Hoch, J. L. Rubenstein, S. Pleasure, Genes and signaling events that establish regional patterning of the mammalian forebrain. *Semin. Cell Dev. Biol.* **20**, 378–386 (2009).
50. Y. Ohkubo, C. Chiang, J. L. Rubenstein, Coordinate regulation and synergistic actions of BMP4, SHH and *FGF8* in the rostral prosencephalon regulate morphogenesis of the telencephalic and optic vesicles. *Neuroscience* **111**, 1–17 (2002).
51. C. C. Winkler *et al.*, The dorsal wave of neocortical oligodendrogenesis begins embryonically and requires multiple sources of sonic hedgehog. *J. Neurosci.* **38**, 5237–5250 (2018).
52. Y. Zhang *et al.*, Cortical neural stem cell lineage progression is regulated by extrinsic signaling molecule sonic hedgehog. *Cell Rep.* **30**, 4490–4504.e4 (2020).
53. O. R. Yabut *et al.*, The neocortical progenitor specification program is established through combined modulation of SHH and *FGF* signaling. *J. Neurosci.* **40**, 6872–6887 (2020).
54. S. Govindan, P. Oberst, D. Jabaudon, In vivo pulse labeling of isochronic cohorts of cells in the central nervous system using FlashTag. *Nat. Protoc.* **13**, 2297–2311 (2018).
55. D. J. Di Bella *et al.*, Molecular logic of cellular diversification in the mouse cerebral cortex. *Nature* **595**, 554–559 (2021).
56. N. Micali *et al.*, Variation of human neural stem cells generating organizer states in vitro before committing to cortical excitatory or inhibitory neuronal fates. *Cell Rep.* **31**, 107599 (2020).
57. L. Ma *et al.*, Developmental programming and lineage branching of early human telencephalon. *Embo J.* **40**, e107277 (2021).
58. H. J. Kim, D. Bar-Sagi, Modulation of signalling by Sprouty: A developing story. *Nat. Rev. Mol. Cell Biol.* **5**, 441–450 (2004).
59. X. Heng, Q. Guo, A. W. Leung, J. Y. Li, Analogous mechanism regulating formation of neocortical basal radial glia and cerebellar Bergmann glia. *Elife* **6**, e23253 (2017).
60. A. E. Trevino *et al.*, Chromatin and gene-regulatory dynamics of the developing human cerebral cortex at single-cell resolution. *Cell* **184**, 5053–5069.e23 (2021).
61. I. Reillo *et al.*, A complex code of extrinsic influences on cortical progenitor cells of higher mammals. *Cereb. Cortex* **27**, 4586–4606 (2017).
62. W. D. Jones, S. M. Gadiana, E. A. Grove, A model of neocortical area patterning in the lissencephalic mouse may hold for larger gyrencephalic brains. *J. Comp. Neurol.* **527**, 1461–1477 (2019).
63. T. Ma *et al.*, Subcortical origins of human and monkey neocortical interneurons. *Nat. Neurosci.* **16**, 1588–1597 (2013).
64. C. Wang *et al.*, Human and monkey striatal interneurons are derived from the medial ganglionic eminence but not from the adult subventricular zone. *J. Soc. Neurosci.* **34**, 10906–10923 (2014).
65. A. M. Pani *et al.*, Ancient deuterostome origins of vertebrate brain signalling centres. *Nature* **483**, 289–294 (2012).
66. N. Micali *et al.*, Molecular programs of regional specification and neural stem cell fate progression in macaque telencephalon. *Science* **382**, eadf3786 (2023).
67. E. Braun *et al.*, Comprehensive cell atlas of the first-trimester developing human brain. *Science* **382**, eadf1226 (2023).

68. I. Kelava, E. Lewitus, W. B. Huttner, The secondary loss of gyrencephaly as an example of evolutionary phenotypical reversal. *Front. Neuroanat.* **7**, 16 (2013).
69. C. C. Hui, S. Angers, Gli proteins in development and disease. *Annu. Rev. Cell Dev. Biol.* **27**, 513–537 (2011).
70. B. Wang, J. F. Fallon, P. A. Beachy, Hedgehog-regulated processing of Gli3 produces an anterior/posterior repressor gradient in the developing vertebrate limb. *Cell* **100**, 423–434 (2000).
71. M. C. Tiveron, H. Cremer, CXCL12/CXCR4 signalling in neuronal cell migration. *Curr. Opin. Neurobiol.* **18**, 237–244 (2008).
72. R. S. Klein *et al.*, SDF-1 alpha induces chemotaxis and enhances Sonic hedgehog-induced proliferation of cerebellar granule cells. *Development* **128**, 1971–1981 (2001).
73. A. M. E. Walenkamp, C. Lapa, K. Herrmann, H. J. Wester, CXCR4 ligands: The next big hit? *J. Nucl. Med.* **58**, 77S–82S (2017).
74. R. Rao, R. Salloum, M. Xin, Q. R. Lu, The G protein Galphas acts as a tumor suppressor in sonic hedgehog signaling-driven tumorigenesis. *Cell Cycle* **15**, 1325–1330 (2016).
75. M. P. Lun *et al.*, Spatially heterogeneous choroid plexus transcriptomes encode positional identity and contribute to regional CSF production. *J. Neurosci.* **35**, 4903–4916 (2015).
76. X. Huang *et al.*, Sonic hedgehog signaling regulates a novel epithelial progenitor domain of the hindbrain choroid plexus. *Development* **136**, 2535–2543 (2009).
77. Y. Fu *et al.*, Heterogeneity of glial progenitor cells during the neurogenesis-to-gliogenesis switch in the developing human cerebral cortex. *Cell Rep.* **34**, 108788 (2021).
78. X. Zhang *et al.*, Bulk and mosaic deletions of Egrf reveal regionally defined gliogenesis in the developing mouse forebrain. *iScience* **26**, 106242 (2023).
79. T. Hara, K. Tanegashima, CXCL14 antagonizes the CXCL12–CXCR4 signaling axis. *Biomol. Concepts* **5**, 167–173 (2014).
80. K. R. Jessen, Glial cells. *Int. J. Biochem. Cell Biol.* **36**, 1861–1867 (2004).
81. P. H. Crossley, S. Martinez, Y. Ohkubo, J. L. Rubenstein, Coordinate expression of Fgf8, Otx2, Bmp4, and Shh in the rostral prosencephalon during development of the telencephalic and optic vesicles. *Neuroscience* **108**, 183–206 (2001).
82. D. M. Ornitz, L. Legeai-Mallet, Achondroplasia: Development, pathogenesis, and therapy. *Dev. Dyn.* **246**, 291–309 (2017).
83. R. F. Hevner, The cerebral cortex malformation in thanatophoric dysplasia: Neuropathology and pathogenesis. *Acta Neuropathol.* **110**, 208–221 (2005).
84. R. E. Thomson, F. Pellicano, T. Iwata, Fibroblast growth factor receptor 3 kinase domain mutation increases cortical progenitor proliferation via mitogen-activated protein kinase activation. *J. Neurochem.* **100**, 1565–1578 (2007).
85. A. Yasoda *et al.*, Overexpression of CNP in chondrocytes rescues achondroplasia through a MAPK-dependent pathway. *Nat. Med.* **10**, 80–86 (2004).
86. A. Alzu'bi *et al.*, The transcription factors COUP-TFI and COUP-TFII have distinct roles in arealisation and GABAergic interneuron specification in the early human fetal telencephalon. *Cereb. Cortex* **27**, 4971–4987 (2017).
87. C. de Juan Romero, C. Bruder, U. Tomasello, J. M. Sanz-Anquela, V. Borrell, Discrete domains of gene expression in germinal layers distinguish the development of gyrencephaly. *Embo J.* **34**, 1859–1874 (2015).
88. L. Wang, S. Hou, Y. G. Han, Hedgehog signaling promotes basal progenitor expansion and the growth and folding of the neocortex. *Nat. Neurosci.* **19**, 888–896 (2016).
89. L. Zhang *et al.*, Counter-balance between Gli3 and miR-7 is required for proper morphogenesis and size control of the mouse brain. *Front. Cell Neurosci.* **12**, 259 (2018).
90. W. Shao *et al.*, Centrosome anchoring regulates progenitor properties and cortical formation. *Nature* **580**, 106–112 (2020).
91. A. Roy *et al.*, PI3K-Yap activity drives cortical gyrification and hydrocephalus in mice. *Elife* **8**, e45961 (2019).